

Synthesis, Characterization, and Properties of Three Europium 2-Propoxides: $[\text{Eu}_4(\text{OPr}^i)_{10}(\text{HOPr}^i)_3] \cdot 2\text{HOPr}^i$, $\text{Eu}_5\text{O}(\text{OPr}^i)_{13}$, and $\text{EuAl}_3(\text{OPr}^i)_{12}$

G. Westin,^{*†} M. Moustiakimov,[‡] and M. Kritikos[‡]

Department of Materials Chemistry, Ångström Laboratory, Uppsala University, SE-751 21 Uppsala, Sweden, and Department of Structural Chemistry, Arrhenius Laboratory, Stockholm University, SE-106 91 Stockholm, Sweden

Received July 12, 2001

The reaction of Eu metal with HOPrⁱ/toluene solutions yielded the mixed Eu²⁺/Eu³⁺ alkoxide $[\text{Eu}_4(\text{OPr}^i)_{10}(\text{HOPr}^i)_3] \cdot 2\text{HOPr}^i$ (**1**), in contrast to the other lanthanide metals, which exclusively yield trivalent lanthanide ions in the alkoxides formed. Metathesis between EuCl₃ and 3KOPrⁱ and stoichiometric hydrolysis yielded the square-pyramidal $\text{Eu}_5\text{O}(\text{OPr}^i)_{13}$ (**2**), and metathesis with EuCl₃ and 3KAl(OPrⁱ)₄ gave $\text{EuAl}_3(\text{OPr}^i)_{12}$ (**3**). The structures of these compounds were determined by single-crystal X-ray diffraction. IR spectroscopic studies showed that the solid-state molecular structure of the three alkoxides remained close to intact in solution. Further characterizations were made with UV–vis spectroscopy, differential scanning calorimetry, and solubility studies. It was also found that **1** can be converted to **2** by oxidation with dioxygen, but **2** was not reduced by Eu metal to **1**. The reactions of **2** and **1** with Al₄(OPrⁱ)₁₂ in toluene/HOPrⁱ solvent were studied by IR and UV–vis spectroscopy; **2** reacted completely to form **3** in 2 h at 75 °C, while **1** reacted to yield **3** and other unidentified Eu²⁺ containing product(s) in the same time.

1. Introduction

In the organic sol–gel processing of high-tech ceramic materials, alkoxides are the most important precursors.¹ Knowledge about their structures is important for the understanding of the sol–gel process itself and for giving increased possibilities of tailoring the product content and morphology. An area that has received considerable interest in recent time is the sol–gel processing of rare-earth doped glasses and ceramics as bulk, waveguide, and finely powdered material. In these materials, lanthanide ion doping produces ceramics that can be used in a number of applications, for example, for laser amplification and frequency up-conversion in the near-IR region, for signal enhancement in integrated optic devices, and in various types of fluorescent lamps and displays.^{2,3} In the latter application, Eu doping is of great importance.

The purest materials and lowest preparation temperatures are normally obtained with the very reactive alkyl-alkoxides

or ether-oxygen containing alkyl-alkoxides, in many cases also containing oxo-ligands, but the number of such Eu alkoxides whose structures have been determined is, as far as we can find, limited to $\text{EuNa}_8(\text{OH})(\text{O}^i\text{Bu})_{10}$ ⁴ and $\text{EuSn}_2(\text{O}^i\text{Bu})_6$.⁵ In the 1970s, Mazdiyasnı et al. reported the formation of Eu 2-propoxide by dissolution of the metal with a mercury salt as catalyst in 2-propanol containing solvents at reflux.⁶ The Eu alkoxide was assumed to have the formula $\text{Eu}(\text{OPr}^i)_2$, on the basis of IR and elemental analysis data.⁶ During the course of our studies, Evans et al. reported that a divalent Eu 2-propoxide formed by dissolution of metal

* To whom correspondence should be addressed. E-mail: Gunnar.Westin@mkem.uu.se.

† Uppsala University.

‡ Stockholm University.

(1) Chandler, C. D.; Rogers, C.; Hampden-Smith, M. J. *Chem. Rev.* **1993**, *93*, 1205. Brinker, C. J.; Scherer, G. W. *The Physics and Chemistry of Sol–Gel Processing*; Academic Press: London, 1990.

(2) Weber, M. J. *J. Non-Cryst. Solids* **1990**, *123*, 208. Westin, G.; Ekstrand, A.; Zanghellini, E.; Börjesson, L. *J. Phys. Chem. Solids* **2000**, *61*, 67. Yeh, D. C.; Sibley, W. A.; Suscavage, M.; Drexhage, M. G. *J. Appl. Phys.* **1987**, *62*, 266. Shinn, M. D.; Sobley, W. A.; Drexhage, M. G.; Brown, R. N. *Phys. Rev.* **1983**, *27*, 6635. Desurvire, E. *Phys Today* **1994**, *16*, 20.

(3) Nageno, Y.; Takebe, H.; Morinaga, K.; Izumitani, T. *J. Non-Cryst. Solids* **1994**, *169*, 288. Piriou, B.; Chen, Y. F.; Vilminot, S. *Eur. J. Solid State Inorg. Chem.* **1998**, *35*, 341. Pillonet-Minardi, A.; Marty, O.; Bovier, C.; Carapon, C.; Mugnier, J. *Opt. Mater. (Amsterdam)* **2001**, *16*, 9.

(4) Evans, W. J.; Sollenberger, M. S.; Ziller, J. W. *J. Am. Chem. Soc.* **1993**, *115*, 4120.

(5) Veith, M.; Hans, J.; Stahl, L.; May, P.; Huch, V.; Sebald, A. *Z. Naturforsch., B: Chem. Sci.* **1991**, *46*, 403.

(6) Brown, L. M.; Mazdiyasnı, K. S. *Inorg. Chem.* **1970**, *9*, 2783.

without catalyst at temperatures up to 45 °C which, after dissolution in THF and crystallization, yielded a product formulated as $\text{Eu}(\text{OPr}^i)_2(\text{THF})_x$. Refluxing in HOPr^i yielded instead mixed $\text{Eu}^{2+}/\text{Eu}^{3+}$ compounds.⁷ Evans et al. also reported the synthesis of a methoxy-ethoxide formulated as $\text{Eu}(\text{OC}_2\text{H}_4\text{OCH}_3)_2$ by dissolution of Eu metal in methoxy-ethanol.⁸ Unfortunately, it has proven difficult to obtain the crystal structures of the homometallic Eu alkoxides, and so far, no structure has been reported for any of these compounds.

In the present work, which is part of a larger study on homo- and heterometallic Ln alkoxides,^{9–16} we obtained as the product of metal dissolution in HOPr^i the mixed-valence alkoxide **1**, rather than the expected trivalent Eu alkoxide **2**. The latter compound can be however obtained by metathesis of EuCl_3 and KOPr^i , combined with stoichiometric hydrolysis. Compound **1** could also be converted to **2** by oxidation with O_2 , while we failed to reduce **2** by Eu metal to **1**. Furthermore, the reaction in solution of both these 2-propoxides with $\text{Al}_4(\text{OPr}^i)_{12}$ to yield **3** was studied. This reaction is intriguing since it has been reported by several groups not to occur with $\text{Ln} = \text{Sc}, \text{Y},$ and $\text{Nd}^{17–19}$ even under reflux, but has worked in our hands with $\text{Ln} = \text{Y}, \text{Er}, \text{Gd},$ and $\text{Nd}^{9,10}$. The structures of the three mentioned Eu alkoxides were determined by single-crystal X-ray techniques, and they were characterized by differential scanning calorimetry, IR and UV–vis spectroscopy, and solubility studies.

2. Experimental Section

2.1. Equipment and Chemicals. The elemental ratios (Eu, K, Cl, and Hg) were obtained from samples hydrolyzed in air and gently dried, using a scanning electron microscope (SEM, JEOL 820) equipped for analysis of energy-dispersive X-ray spectra (EDS, LINK AN 10000). The presence of these elements can normally be detected down to ~0.3 at. %. FT-IR spectra, in the range 5000–370 cm^{-1} , were recorded with a Bruker IFS-55 spectrometer, with solid samples as KBr tablets and paraffin mulls and dissolved samples in a 0.1 mm path-length KBr cell. UV–vis spectra, in the range 300–800 nm, were obtained at ambient temperature with a Perkin-Elmer Lambda 19 dispersive spectrometer with a <0.3 nm slit. The solutions were analyzed in sealed quartz cuvettes, and the

solid materials, in transmittance mode, placed in quartz cuvettes in front of a 60 mm integrated reflectance sphere. Up to 50 scans were collected to obtain sufficiently good average signal-to-noise ratio. The behavior on heating in the range 25–250 °C, at a rate of 5 °C min^{-1} , was studied with a differential scanning calorimeter (DSC, Perkin-Elmer DSC-2), using airtight steel compartments. Crystals in sealed glass capillaries were visually studied during heating, using a solid-block melting-point apparatus at temperatures up to 300 °C.

The syntheses and recrystallizations, as well as the preparations of samples for DSC, IR and UV–vis spectroscopic, and visual studies during heating, and the mounting of crystals for single-crystal X-ray data collection, were performed in a glovebox containing dry, oxygen-free argon atmosphere. The europium metal was dissolved outside the glovebox, in closed vessels connected to an isopiestic nitrogen atmosphere dried with P_2O_5 . The oxygen gas used in the oxidation experiments was dried with P_2O_5 . The glassware was dried at 150 °C for more than 30 min before being inserted into the glovebox. The toluene and the 2-propanol (HOPr^i) were dried by distillation over CaH_2 . Eu metal (99.9% Strem Chemicals) and anhydrous EuCl_3 (99.9% Strem Chemicals) were used as purchased. Commercial $\text{Al}_4(\text{OPr}^i)_{12}$ (Aldrich or Sigma) was recrystallized before use.

2.2. Synthesis. $[\text{Eu}_4(\text{OPr}^i)_{10}(\text{HOPr}^i)_3] \cdot 2\text{HOPr}^i$ (1**).** Typically, 13.61 mmol (2.000 g) of Eu metal was added a 1:1 mixture (vol/vol) of 40 mL of toluene and HOPr^i . A small amount (~1 mg, 0.004 mmol) of HgCl_2 was added as catalyst. This mixture was heated to 65–70 °C and reacted for 24 h to dissolve the metal. The dark yellow solution was transferred to another beaker, leaving behind a very small amount of black powder. Slow evaporation of the solvent produced an orange-yellow mass of small crystals of **1**, in a yield of 98% based on Eu. SEM-EDS studies showed no impurities of Hg and Cl in the product. Larger crystals for X-ray determination were prepared by dissolving the crystal mass in HOPr^i and very slowly evaporating the solvent. IR and UV–vis spectra of the compound are given in Figures 1 and 2, respectively. Selected peaks for identification: IR(KBr) 1174sh, 1165, 1132, 1000, 970, 832sh, 822, 520, 484, 444, 413, 398 cm^{-1} ; and UV–vis(HOPr^i) 526.3, 530.9, 539.8, 578.7, 584 nm. Compound **1** is very soluble in HOPr^i and rather soluble in toluene and hexane, which is rather unusual for alkoxides. It is stable for long times in HOPr^i and in the solid state.

$\text{Eu}_5\text{O}(\text{OPr}^i)_{13}$ (2**).** Typically, 12.8 mmol (0.500 g) of K was dissolved in 20 mL of 1:1 (vol/vol) toluene/ HOPr^i , and 0.85 mL of 1 M H_2O in toluene/ HOPr^i was added. Then, 4.263 mmol (1.101 g) of EuCl_3 was added, and after 48 h at room temperature, the mixture was centrifuged to separate the white precipitate of KCl formed in the reaction. The very pale yellow solution part was evaporated to dryness, and just enough toluene was added to dissolve it, and then, crystallization was achieved by slow evaporation. The yield of the off-white, transparent crystals of **2** was 90%. SEM-EDS analyses showed no signals from K or Cl. IR and UV–vis spectra of the compound are shown in Figures 5 and 6, respectively. Selected peaks for identification: IR(KBr) 1164, 1151sh, 1130, 1125, 1001, 975, 970sh, 957sh, 953, 837, 829sh, 824, 526, 490, 446, 435sh, 417sh, 409, 396sh, 389sh, 384, 380 cm^{-1} ; and UV–vis(toluene/ HOPr^i 1:2) 376.4, 378.1, 381, 384.8, 390.8, 399.5, 401.4, 411, 412.9, 462.4, 464.4, 524.8, 532.8, 576.5, 583.2, 587 nm. Compound **2** is very soluble in toluene and hexane but is only slightly soluble in HOPr^i . The compound is stable for long times in any of these solvents or in the solid state.

$\text{EuAl}_3(\text{OPr}^i)_{12}$ (3**).** Typically, 12.8 mmol (0.500 g) of K was dissolved in 35 mL of 1:2 (vol/vol) toluene/ HOPr^i , followed by

- (7) Evans, W. J.; Greci, M. A.; Ziller, J. W. *Inorg. Chem.* **2000**, *39*, 3213.
 (8) Evans, W. J.; Greci, M. A.; Ziller, J. W. *Inorg. Chem.* **1998**, *37*, 5221.
 (9) Westin, G.; Kritikos, M.; Wijk, M. *J. Solid State Chem.* **1998**, *141*, 168.
 (10) Kritikos, M.; Moustiakimov, M.; Wijk, M.; Westin, G. *J. Chem. Soc., Dalton Trans.* **2001**, *13*, 1931.
 (11) Wijk, M.; Norrestam, R.; Nygren, M.; Westin, G. *Inorg. Chem.* **1996**, *35*, 1077.
 (12) Westin, G.; Wijk, M.; Moustiakimov, M.; Kritikos, M. *J. Sol-Gel Sci. Technol.* **1998**, *13*, 125.
 (13) Moustiakimov, M.; Kritikos, M.; Westin, G., *Acta Crystallogr.* **2001**, *C57*, 515.
 (14) Wijk, M.; Kritikos, M.; Westin, G. *Acta Crystallogr.* **1998**, *C54*, 576.
 (15) Westin, G.; Norrestam, R.; Nygren, M.; Wijk, M. *J. Solid State Chem.* **1998**, *135*, 149.
 (16) Moustiakimov, M.; Kritikos, M.; Westin, G. *Acta Crystallogr.* **1998**, *C54*, 29.
 (17) Turevskaya, E. P.; Belokon, A. I.; Starikova, Z. A.; Yanovsky, A. I.; Kiruschenkov, E. N.; Turova, N. Ya. *Polyhedron* **2000**, *19*, 705.
 (18) Poncelet, O.; Sartain, W. J.; Hubert-Pfalzgraf, L. G.; Folting, K.; Caulton, K. G. *Inorg. Chem.* **1989**, *28*, 263.
 (19) Helgesson, G.; Jagner, S.; Poncelet, O.; Hubert-Pfalzgraf, L. G. *Polyhedron* **1991**, *10*, 1559.

Table 1. Selected Crystal Data for $\text{Eu}_4(\text{OPr}^i)_{10}(\text{HOPr}^i)_3 \cdot 2(\text{HOPr}^i)$ (**1**), $\text{Eu}_5\text{O}(\text{OPr}^i)_{13}$ (**2**), and $\text{EuAl}_3(\text{OPr}^i)_{12}$ (**3**)

	1	2	3
empirical formula	$\text{C}_{45}\text{H}_{110}\text{O}_{15}\text{Eu}_4$	$\text{C}_{39}\text{H}_{91}\text{O}_{14}\text{Eu}_5$	$\text{C}_{36}\text{H}_{84}\text{O}_{12}\text{Al}_3\text{Eu}$
fw	1499.17	1543.92	941.93
cryst syst	monoclinic	monoclinic	monoclinic
space group	$P2_1/n$ (No. 14)	$P2_1/n$ (No. 14)	$P2_1$ (No. 4)
<i>a</i> , Å	23.246(5)	12.846(17)	13.146(2)
<i>b</i> , Å	22.372(5)	21.54(3)	22.738(2)
<i>c</i> , Å	27.466(6)	21.65(2)	16.971(3)
β , deg	108.30(2)	91.49(10) ^o	90.00(0) ^o
<i>V</i> , Å ³	13562(5)	5990(12)	5072.8(13)
<i>Z</i>	8	4	4
ρ_{calc} , g cm ⁻³	1.469(1)	2.112(1)	1.233(1)
temp, K	150(2)	170(1)	120(2)
$\mu(\text{Mo K}\alpha)$, (mm ⁻¹)	3.697	5.206	1.336
<i>F</i> (000)	6016.0	3008.0	1992.0
<i>N</i> (obs)/ <i>N</i> (par)/ <i>N</i> (res)	7833/855/32	3888/325/29	10401/925/7
R1, wR2, (<i>I</i> > 2 σ (<i>I</i>)) ^a	0.0611, 0.1441	0.0797, 0.2171	0.0336, 0.0924
$\Delta\rho_{\text{max}}$, $\Delta\rho_{\text{min}}$ (e/Å ³)	1.04, -1.17	1.55, -1.14	0.45, -0.88

$$^a \text{R1} = \sum ||F_o| - |F_c|| / \sum |F_o|; \text{wR2} = [\sum [w(F_o^2 - F_c^2)^2] / \sum [w(F_o^2)^2]]^{1/2}.$$

addition of 12.8 mmol (2.612 g) $\text{Al}(\text{OPr}^i)_3$. Two hours later, 4.263 mmol (1.101 g) of EuCl_3 was added. After another 48 h at room temperature, the mixture was centrifuged to separate the white precipitate of KCl formed in the reaction. The solution part was evaporated to dryness, and just enough toluene was added to dissolve it, before crystallization was achieved by slow evaporation. The off-white crystals formed were then washed with a small amount of HOPr^i . The yield of **3** was ~90%. The SEM-EDS analyses showed that the Eu/Al ratio was correct and no K or Cl was present within the expected error. IR spectra and UV-vis spectra of the compound are shown in Figures 8 and 9, respectively. Selected peaks for identification: IR(KBr) 1200sh, 1185, 1171, 1159sh, 1138, 1126, 1120sh, 1042sh, 1034, 958sh, 954, 862, 856, 830, 730, 669, 608, 587sh, 573, 539, 477, 461sh, 448, 430sh, 401 cm⁻¹; and UV-vis(hexane) 362.4, 375.0, 376.9, 378.6, 381.3, 383.5, 391.8, 393.9, 396.1, 401.0, 402.3, 410.7, 417.4, 419.0, 460.8, 463.5, 466.0, 524.0sh, 525.8, 528.2sh, 529.5, 532.3, 537.1, 574.6, 576.5, 583.7, 593.4 nm. Compound **3** is very soluble in toluene and hexane but is only slightly soluble in HOPr^i . The compound is stable for long times in any of these solvents or in the solid state.

2.3. Structure Determinations. Suitable single crystals of **1**, **2**, and **3** were selected and glued with a very small amount of paraffin in glass capillaries that were subsequently melt sealed. Single-crystal X-ray diffraction data were collected on a Stoe image-plate diffractometer at low temperature. Selected crystallographic and experimental data for **1**, **2**, and **3**, together with the refinement details, are given in Table 1. Systematic absences in the collected diffraction data were consistent with space groups $P2_1/n$ (No. 14) for **1** and **2** and $P2_1$ (No. 4) for **3**. The data were corrected for absorption effects using the X-Shape program package.²⁰ The structures were solved with direct methods and refined against F^2 with the computer programs SHELXS97²¹ and SHELXL97,²² respectively. Hydrogen atoms were added at ideal positions and refined using a riding model with thermal displacement parameters 1.2 times the U_{iso} of their respective pivot carbons. The absolute configuration for noncentrosymmetric **3** was chosen according to the Flack parameter (-0.049). The investigated crystal was pseudomerohedrally twinned with the twin law: 100, 0 $\bar{1}$ 0, 00 $\bar{1}$.

The twin fraction was refined to 0.497 and subsequently fixed at 0.5. A number of 2-propyl groups in all three structures appeared to be disordered. Further details on the refinement are provided as Supporting Information.

3. Results and Discussion

3.1. $[\text{Eu}_4(\text{OPr}^i)_{10}(\text{HOPr}^i)_3] \cdot 2\text{HOPr}^i$ (1**). Synthesis.** The europium metal was dissolved in toluene/ HOPr^i (1:1) in close accordance with the synthesis routes reported by Brown and Mazdiyasi et al.⁶ and by Evans et al.⁷ The former group obtained a product formulated as $\text{Eu}(\text{OPr}^i)_2$, while the latter group reported the formation of a divalent Eu 2-propoxide when using temperatures up to 45 °C without catalysis, and mixed $\text{Eu}^{2+}/\text{Eu}^{3+}$ products when using reflux temperature.

The product of our synthesis was the same with or without Hg catalyst and regardless of temperature in the studied interval 25–70 °C. It is possible that our Eu 2-propoxide is identical with that reported by Evans et al., but more data are needed for a safe conclusion. The structural determination showed that the mixed $\text{Eu}^{2+}/\text{Eu}^{3+}$ valence alkoxide **1** formed, and IR spectroscopic studies, as well as the homogeneous color and shape of the small crystals, indicated that the compound was highly pure and monophasic. The isolated yield was 98%, which is much higher than that for dissolution of the other lanthanide metals under the same conditions; the normal yield is some 45%–75% of isolated alkoxide.^{6,9,10,18,23,24} After dissolution of the Eu metal, a very small amount of a black, insoluble material remained, which might come from some parts of the Eu metal pieces where the oxide layer was not entirely removed, or from Hg/Eu/Cl residues. In contrast, a large amount of very fine olive-green particles, shown to be Ln hydride, formed in an amount of ~50 mol % with the other lanthanide metals.^{9,23} The difference between Eu and the other Ln metals is that the dissolution proceeds through a divalent state for Eu, which seems to prevent hydride formation, whereas no divalent alkoxides of the other lanthanide elements (Lu–Sm, Pr–La) have been observed under similar conditions.

IR Spectroscopy. The IR spectrum of **1** is shown in Figure 1. The peak maxima in the fingerprint region, 1200–370 cm⁻¹, are assigned to 1200–800 cm⁻¹ C–O and C–C stretch; 850–800 cm⁻¹ C–O and C–C bend; and 550–370 cm⁻¹ Eu–O stretch. A hydroxyl stretch band with a maximum at 3210 and a shoulder at 3340 cm⁻¹, tailing down to ~2100 cm⁻¹, indicated a variety of hydrogen bonds ranging from strong to weak, which is consistent with the structure determination. The IR spectra of solid and dissolved **1** are quite similar, indicating that the molecular entities remain almost unchanged in solution. In the hexane solution, the OH stretch maximum was found at 3350 cm⁻¹ which fits the shoulder of the solid-state compound well, but the peak at 3210 cm⁻¹ was much reduced in intensity, and the long tail to 2100 cm⁻¹ was missing. This indicates that the stronger hydrogen bonds had been destroyed, perhaps the bonds between HOPr^i molecules binding the Eu complexes

(20) STOE, X-SHAPE revision 1.09. Crystal Optimisation for Numerical Absorption Correction; Darmstadt, 1997.

(21) Sheldrick, G. M. *Acta Crystallogr.* **1994**, A46, 467.

(22) Sheldrick, G. M. *SHELXL97. Computer Program for the Refinement of Crystal Structures*, Release 97-2; Sheldrick, G. M., Ed.; University of Göttingen: Göttingen, Germany, 1997.

(23) Westin, G.; Moustiakimov, M.; Kritikos, M. Unpublished results.

(24) Bradley, D. C.; Chudzynska, H.; Frigo, D. M.; Hammond, M. E.; Hursthouse, M. B.; Mazid, M. A. *Polyhedron* **1990**, 9, 719.

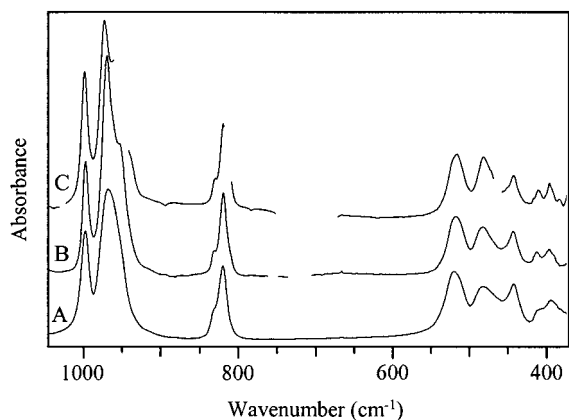


Figure 1. IR spectra of **1** as solid in KBr (A), hexane solution (B), and toluene/HOPr³ (1:2) solution (C).

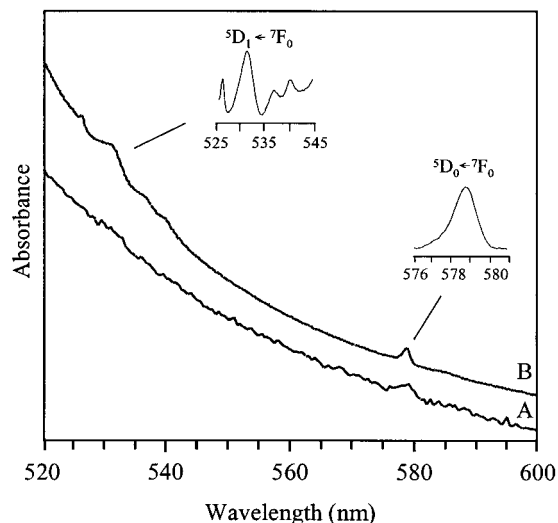


Figure 2. Electronic spectra of **1** as solid (A) and HOPr³ solution (B). (The insert picture spectrum of the of the ${}^5D_1 \leftarrow {}^7F_0$ transition has been baseline corrected with a straight line.)

together. In addition, a sharp peak at 3637 cm^{-1} was observed, indicating isolated HOPr³ molecules.

UV–Vis Spectroscopy. The electronic transition spectra of solid and dissolved **1** are shown in Figure 2. The spectra contain a very strong band stretching from the UV region to $\sim 550\text{--}600\text{ nm}$, causing the strong orange-yellow color of the compound. We have earlier shown that the fine structure of the absorptions in the UV–vis–NIR region can be used to study even very subtle changes in the coordination geometry of Ln³⁺ ions, making it possible to separate different Ln³⁺ ion sites, even with the same coordination number and only oxygen donor ligands.^{9,10,15} Also, Eu³⁺ is suitable for such studies, and the assignments have been made according to the scheme reported by Yatsimirskii et al.³³ Five weak peaks, assigned as due to f–f transitions within the Eu³⁺ ions, can be observed in the solution

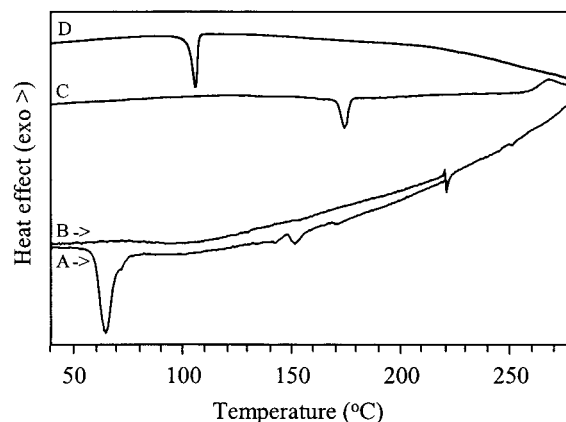


Figure 3. DSC graphs of **1** as a fresh sample (A) and a sample reheated, after first being heated to $220\text{ }^\circ\text{C}$ and cooled (B), **2** (C), and **3** (D).

spectrum, but it was not possible to obtain well-defined peaks from the solid material.

Behavior on Heating. Inspection of crystals in sealed glass capillaries showed that the compound melted to a clear yellow liquid at $55\text{--}58\text{ }^\circ\text{C}$, followed by some bubbling in the range $80\text{--}130\text{ }^\circ\text{C}$, leaving a solid yellow material. No major changes were observed on further heating to about $250\text{ }^\circ\text{C}$ where the material darkened. In the DSC graph, shown in Figure 3, a composite endothermic peak is observed in the interval $52\text{--}74\text{ }^\circ\text{C}$ which coincides with the observed melting of the compound. This shape of this composite peak differed much more between different samples than is usual, but the distribution of enthalpies of it was found to be normal, $\sim 40\text{--}50\text{ kJ mol}^{-1}$. The composite negative peaks observed in four runs of samples, kept at ambient temperature before the runs, always had a main peak with an onset of $53\text{--}57\text{ }^\circ\text{C}$ and a minimum of $59\text{--}61\text{ }^\circ\text{C}$, as that observed in Figure 3. In addition to this peak, a shoulder on the low-temperature side starting at $\sim 40\text{ }^\circ\text{C}$ and/or a shoulder on the high-temperature side ending at $\sim 75\text{ }^\circ\text{C}$ was observed in some runs. A sample kept at $-30\text{ }^\circ\text{C}$ before the run had even stronger peaks before and after the main peak. This endotherm coincides with the observed melting of the compound, but the negative enthalpy is somewhat higher than is normal for melting alone, which is normally found around $5\text{--}20\text{ kJ mol}^{-1}$,^{9,10} and the number of closely spaced peaks indicate a more complex process. It might be speculated that the peaks stem from a melting occurring after the intermolecular hydrogen bonds have been broken up and followed by some rearrangements of the HOPr³ molecules. This might be similar to what happens on dissolution of **1**, where the IR study indicated changes mainly in the hydrogen bonds and virtually unchanged Eu–O bonds within the complex clusters. It is also possible that some of the HOPr³ molecules are released even at this low temperature and contribute by dissolving the complexes. The bubbling observed following

(25) Sirio, C.; Hubert-Pfalzgraf, L. G.; Bois, C. *Polyhedron* **1997**, *16*, 1129.
 (26) Clegg, W.; Drummond, A. M.; Liddle, S. T.; Mulvey, R. E.; Robertson, A. *Chem. Commun.* **1999**, 1569.
 (27) Turevskaya, E. P.; Turova, N. Ya.; Kessler, V. G.; Yanovsky, A. I.; Struchkov, Yu. T. *Zh. Neorg. Khim.* **1993**, *38*, 928.
 (28) Evans, W. J.; Golden, R. E.; Ziller, J. W. *Inorg. Chem.* **1993**, *32*, 3041.
 (29) Brown, I. D.; Altermatt, D. *Acta Crystallogr.* **1985**, *B41*, 244.

(30) Yunlu, K.; Gradeff, P. S.; Edelstein, N.; Kot, W.; Shalimoff, G.; Streib, W. E.; Vaarstra, B. A.; Caulton, K. G. *Inorg. Chem.* **1991**, *30*, 2317.
 (31) Mehrotra, R. C.; Batwara, M. J. *Inorg. Chem.* **1970**, *9*, 2505.
 (32) Veith, M.; Mathur, S.; Leclerf, N.; Bartz, K.; Heinz, M.; Huch, V. *Chem. Mater.* **2000**, *12*, 271.
 (33) Yatsimirskii, K. B.; Davidenko, N. K. *Coord. Chem. Rev.* **1979**, *27*, 223.

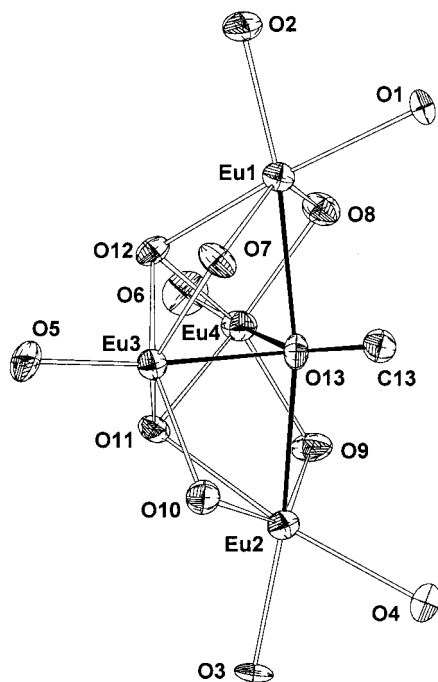


Figure 4. ORTEP view (30% probability displacement ellipsoids) of **1**, showing the molecular structure of the metal–oxygen core. Only one molecule from the asymmetric unit is shown. Note that O13 belongs to a μ_4 -OR group.

the melting above 80 °C is probably due to boiling of the HOPrⁱ. The origins of the low energy transfer ripples around 140 °C are not clearly understood but are possibly due to some sintering of the material observed in some of the visual inspections. The retained yellow color indicates that Eu²⁺ ions remain also after heating to higher temperatures. In a study where the compound had first been heated to 90 or 220 °C, then cooled to room temperature, and then heated again, one could observe that the endotherm was not reproducible, which has been the case also for other solvated alkoxides.^{15,9}

Repeated dissolution of **1** in toluene or hexane followed by evaporation removed the solvating HOPrⁱ molecules according to the IR spectroscopic studies and left a yellowish brown powder different also from **2**. The dark yellow color indicated that the compound still contained Eu²⁺ ions.

Structure. The molecular structure of **1** is shown in Figure 4. Selected bond lengths for **1** are given in Table 2. The asymmetric unit content of this alkoxide consists of two crystallographically independent [Eu₄(OPrⁱ)₁₀(HOPrⁱ)₃] molecules and four HOPrⁱ solvent molecules. The solid-state structure is built up of chains consisting of tetranuclear units that are interconnected with HOPrⁱ molecules. The complexes and the alcohol molecules are connected to each other by hydrogen bonds, resulting in two polymer strands. The two [Eu₄(OPrⁱ)₁₀(HOPrⁱ)₃] molecules have almost identical M₄O₁₃ geometries, and because each of them has two hydrogen-bonded HOPrⁱ solvent molecules in similar arrangements, only one of the tetranuclear molecules will be described here. Further geometrical details for the other molecule can be found in the Supporting Information.

Table 2. Selected Interatomic Distances (Å) for Eu₄(OPrⁱ)₁₀(HOPrⁱ)₃·2(HOPrⁱ) (**1**)

terminal M–O		μ_3 M–O	
Eu(1)–O(1)	2.595(10)	Eu(2)–O(11)	2.595(11)
Eu(1)–O(2)	2.569(12)	Eu(3)–O(11)	2.369(12)
Eu(2)–O(3)	2.500(12)	Eu(4)–O(11)	2.408(10)
Eu(2)–O(4)	2.554(13)	Eu(1)–O(12)	2.538(11)
Eu(3)–O(5)	2.103(11)	Eu(3)–O(12)	2.466(11)
Eu(4)–O(6)	2.100(13)	Eu(4)–O(12)	2.428(10)
μ_2 M–O		μ_4 M–O	
Eu(1)–O(7)	2.452(12)	Eu(1)–O(13)	2.813(11)
Eu(1)–O(8)	2.464(12)	Eu(2)–O(13)	2.801(11)
Eu(2)–O(9)	2.450(12)	Eu(3)–O(13)	2.496(10)
Eu(2)–O(10)	2.503(13)	Eu(4)–O(13)	2.493(12)
Eu(3)–O(7)	2.282(10)		
Eu(3)–O(10)	2.297(11)		
Eu(4)–O(8)	2.283(11)		
Eu(4)–O(9)	2.270(11)		

The four metal atoms form a butterfly conformation in which the metal atoms are connected to each other by two bridging μ_3 -OR and four μ_2 -OR units in addition to the central μ_4 -OR moiety. This μ_4 -OR unit is displaced in the opposite direction compared to the hinge atoms; that is, the Eu(1)–O(13)–Eu(2) angle is 169.5(4)°, which makes the Eu₄(μ_4 -O) unit convex, in contrast to, for example, Ce₄(μ_4 -O) in Ce₄O(OPrⁱ)₁₄,²⁵ where it is concave. The two hinge atoms, Eu(3) and Eu(4), are separated by 3.632(2) Å, while the wingtip atoms, Eu(1) and Eu(2), are separated by 5.591(2) Å. The two distant metal atoms bind two terminal OPrⁱ groups each, while the two other metal atoms bind one terminal OPrⁱ group each.

Quite remarkably, one μ_4 -OPrⁱ group connects all four metal atoms through the O atom. In contrast, the related Ce₄O(OPrⁱ)₁₄ molecule contains a μ_4 -O oxo-oxygen atom in a similar structural position. To our knowledge, this is the first example of a structurally characterized μ_4 -OPrⁱ group. There are, however, known examples of μ_4 -OBu^t²⁶ and μ_4 -OEt²⁷ groups in alkyl-type metal alkoxides and of μ_4 -OpTol²⁸ in the phenoxo ligand group.

The Eu–O bond lengths are in the range 2.45–2.81 Å for the Eu(1) and Eu(2) atoms and between 2.10 and 2.50 Å for Eu(3) and Eu(4). Moreover, there are significant differences between the hinge and wingtip Eu atoms when comparing Eu–OR, Eu– μ_2 -OR, Eu– μ_3 -OR, and Eu– μ_4 -OR distances. The Eu–O bond distance distributions and calculated bond valence sums²⁹ show that the two hinge atoms have oxidation state +3 while the two wingtip atoms are divalent. The presence of Eu²⁺ is also confirmed by the strong yellow color of the solid compound.

The molecular structure of **1** is closely related to several tetranuclear oxo-alkoxides, for example, Ce₄O(OPrⁱ)₁₃-(HOPrⁱ)₃,³⁰ Ce₄O(OPrⁱ)₁₄,²⁵ and Er₂Zr₂O(OPrⁱ)₁₂(HOPrⁱ)₃,¹² but also to the phenoxides, for example, [La₂Na₂(μ_4 -OpTol)(μ_3 -OpTol)₂(μ_2 -OpTol)₄(OpTol)₂(OC₄H₉)₅]^{1–}.²⁸

As mentioned previously, intermolecular hydrogen bonds are present in compound **1**. The 2-propoxo groups involved in hydrogen bonding are located at the wingtip Eu atoms in the butterfly complexes. These terminally bonded 2-propoxo groups have Eu–O–C angles in the range 123°–141°, which are characteristic for 2-propoxo groups participating in

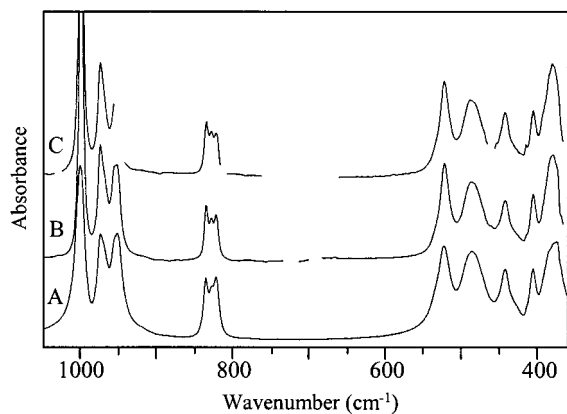


Figure 5. IR spectra of **2** as solid in KBr (A), hexane solution (B), and toluene/HOPrⁱ (2:1) solution (C).

hydrogen bonding. The equivalent angles in the other strand are in the range 134°–140°. Adjacent complexes in both strands are connected to each other through two HOPrⁱ groups. The distances between oxygen atoms involved in hydrogen bonding are slightly different between the two chains, ranging from 2.50(2) to 2.78(2) Å and from 2.53(2) to 2.70(2) Å, respectively. The hydroxylic H atoms necessary for charge balance were not located by the X-ray experiment. The presence of hydrogen bonds ranging from weak to strong was also corroborated by the IR study.

3.2. Eu₅O(OPrⁱ)₁₃ (2**). Synthesis.** After structure determination of the Y and Yb 2-propoxides formed by dissolution of Ln metal, given the formula Ln(OPrⁱ)₃,^{18,24} it was often believed that all isolated Ln 2-propoxides had the Ln₅O(OPrⁱ)₁₃ or Nd₅O(OPrⁱ)₁₃(HOPrⁱ)₂ composition.¹⁹ However, the products of Eu metal dissolution in HOPrⁱ containing solvents have been formulated as Eu(OPrⁱ)₂.^{6,7} The IR spectroscopy data given in the literature for the orange “Eu(OPrⁱ)₂” product reported by Mazdiyasnī et al.⁶ fit most closely to the data of our compound **2**, but in our case, oxidation was necessary to avoid formation of **1**. The orange color reported indicates the presence of at least some Eu²⁺ in the sample, however, but it might also be that the compound was affected differently when subjected to various studies. To get a facile formation of Ln₅O(OPrⁱ)₁₃ (Ln = Er,⁹ Gd,¹⁰ and Nd¹⁰), we have previously used a combination of metathesis and stoichiometric hydrolysis. Using this route to access the pure Eu³⁺ alkoxide, the structure determination of the product showed that **2** was obtained, and IR spectroscopic studies and the homogeneous habit and color of the crystals showed that the compound was highly pure.

IR Spectroscopy. The IR spectrum of the alkoxide is shown in Figure 5; it is consistent with the IR spectra of the other M₅O(OPrⁱ)₁₃ with M = Y, La–Pr, Sm–Lu.²³ The peaks are assigned in the same way as for **1**. The great similarity of the IR spectra of the solid and dissolved compound shows that the molecular structure is retained on dissolution in toluene/HOPrⁱ or hexane solvent.

UV–Vis Spectroscopy. The UV–vis spectra of solid and dissolved **2** are shown in Figure 6. The many weak peaks are assigned as due to transitions between f-orbital levels of Eu³⁺. The peak shapes and positions are very similar in the

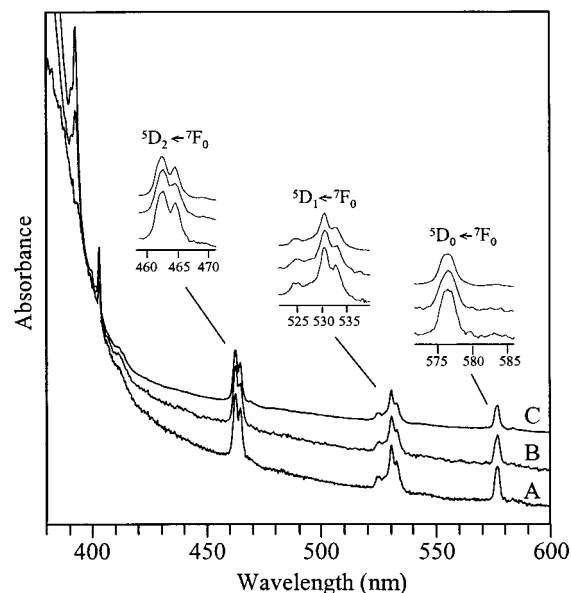


Figure 6. Electronic spectra of **2** as solid (transmittance) (A), hexane solution (B), and toluene/HOPrⁱ (2:1) solution (C).

solid and in solution, which corroborates the indication from the IR spectra of retained structure in solution.

Behavior on Heating. Visual inspection of crystals in melt-sealed glass capillaries showed no changes up to 174 °C, where the crystals became slightly matt. On further heating, no changes were observable up to ~260 °C, where the crystal surfaces started to darken, indicating charring by decomposition of the 2-propyl groups. The DSC graph of **2**, given in Figure 3, shows an endothermic peak with an onset at 168 °C and a minimum at 172 °C, corresponding to an energy of ~10 kJ mol⁻¹. This endotherm is probably due solely to melting, because it could be reproduced after cooling from 180 °C, although melting was not visually observed in glass capillaries. Hence, the behavior of this alkoxide is consistent with the findings on Ln₅O(OPrⁱ)₁₃ (Ln = Er, Nd, Gd).^{9,10}

Structure. Crystallographic data are represented in Table 1. Selected bond lengths and angles are given in Table 3, and the molecular structure is shown in Figure 7. The metal–oxygen M₅O₁₄ fragment of the molecular structure consists of five metal atoms, each of them six-coordinated by oxygen atoms. The five metal atoms form a highly regular square pyramidal polyhedron with the μ₅-O(14) atom displaced 0.22(2) Å above the basal plane. The Eu–O bond distances follow the trend terminal Eu–OR < Eu–μ₂-OR < Eu–μ₃-OR < Eu–μ₅-O. Calculated bond valence sums indicate that the Eu atoms are all trivalent. The Eu–O–C angles are largest for the terminal OR groups (164°–177°); the Eu–O–C angles for the μ₂-OR and μ₃-OR groups are comparable in magnitude to each other (120°–142° and 114°–135°, respectively). The trends seen in bond lengths and angles for **2** are consistent with what is found for other M₅O(OPrⁱ)₁₃ compounds containing the square pyramidal M₅O structure fragment, for example, M = Y,¹⁸ In,²⁴ Yb,²⁴ Er,^{9,10} Gd,¹⁰ Nd.¹⁰ Because the structures of these molecules have been described in detail elsewhere, we omit a more thorough discussion here.

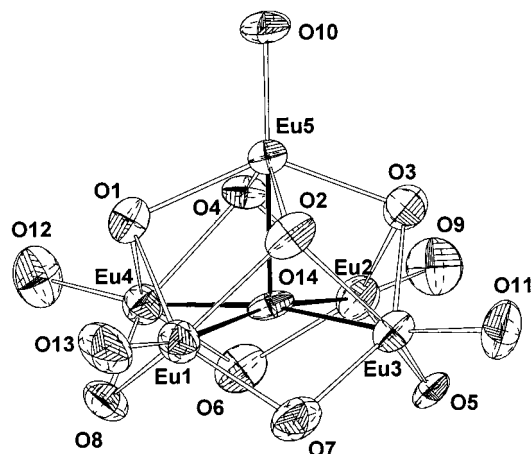
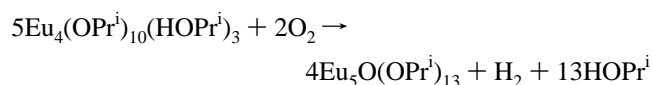
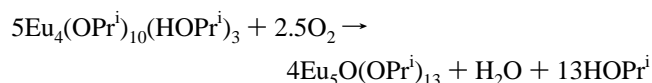


Figure 7. ORTEP view of the metal–oxygen framework of **2** showing 30% probability displacement ellipsoids.

Table 3. Selected Interatomic Distances (Å) for $\text{Eu}_5\text{O}(\text{OPr}^i)_{13}$ (**2**)

terminal M–O		μ_5 M–O	
Eu(1)–O(13)	2.08(2)	Eu(1)–O(14)	2.43(2)
Eu(2)–O(9)	2.06(2)	Eu(2)–O(14)	2.42(2)
Eu(3)–O(11)	2.13(3)	Eu(3)–O(14)	2.41(2)
Eu(4)–O(12)	2.07(2)	Eu(4)–O(14)	2.48(2)
Eu(5)–O(10)	2.07(2)	Eu(5)–O(14)	2.39(2)
μ_2 M–O		μ_3 M–O	
Eu(1)–O(7)	2.27(2)	Eu(1)–O(1)	2.45(2)
Eu(1)–O(8)	2.28(2)	Eu(1)–O(2)	2.48(2)
Eu(2)–O(5)	2.28(2)	Eu(2)–O(3)	2.50(2)
Eu(2)–O(6)	2.31(2)	Eu(2)–O(4)	2.47(2)
Eu(3)–O(5)	2.30(2)	Eu(3)–O(2)	2.46(2)
Eu(3)–O(7)	2.28(2)	Eu(3)–O(3)	2.45(2)
Eu(4)–O(6)	2.28(2)	Eu(4)–O(1)	2.46(2)
Eu(4)–O(8)	2.28(2)	Eu(4)–O(4)	2.42(2)
μ_3 M–O			
Eu(5)–O(1)	2.40(2)		
Eu(5)–O(2)	2.38(2)		
Eu(5)–O(3)	2.36(2)		
Eu(5)–O(4)	2.34(2)		

3.3. Redox Reactions of $[\text{Eu}_4(\text{OPr}^i)_{10}(\text{HOPr}^i)_3] \cdot 2\text{HOPr}^i$ (1**) and $\text{Eu}_5\text{O}(\text{OPr}^i)_{13}$ (**2**). Oxidation of **1**.** The mixed-valence alkoxide, **1**, formed spontaneously when the metal was dissolved under inert atmosphere. Addition of dry oxygen gas to a toluene/HOPrⁱ (1:2) solution or a pure HOPrⁱ solution containing **1** generated a great deal of heat, and the strong yellow color indicating the presence of Eu^{2+} weakened to a very pale yellow tint. The UV–vis and IR spectra showed that the product was almost exclusively **2**. Thus, the Eu^{2+} ions can be oxidized by oxygen gas to yield the exclusively Eu^{3+} containing compound **2**. Two reaction formulas that seem plausible are



The very small amount of byproduct formed indicates that the second formula is a better description of the reactions, which then should occur under relatively reducing conditions.

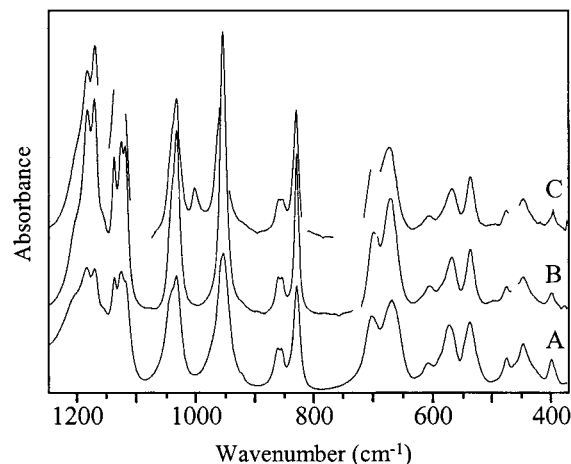
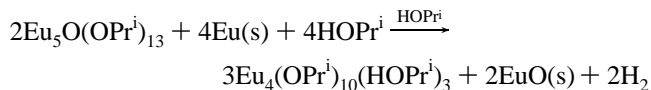


Figure 8. FT-IR spectra of **3** as solid in KBr (A), hexane solution (B), and toluene/HOPrⁱ (2:1) solution (C).

Further oxidation to decompose **2** did not occur even with a large excess of oxygen.

Reduction of 2. An attempt to convert **2** to **1** by reduction and O^{2-} abstraction according to the formula



was made by adding 2 mol of Eu to 1 mol of **2** in toluene/HOPrⁱ (1:1). Within 4 h after mixing the starting compounds, the almost non-colored solution had turned strongly yellow, and some grayish red insoluble material formed. The UV–vis and IR spectra of the evaporated solution part showed that the product was similar to **2**, but not identical, and that it was different from **1**, and thus, the reaction did not proceed as intended.

3.4. $\text{EuAl}_3(\text{OPr}^i)_{12}$ (3**).** Compound **3** was prepared by metathesis in the same way as we prepared $\text{LnAl}_3(\text{OPr}^i)_{12}$ ($\text{Ln} = \text{Er},^{11} \text{Gd},^{10}$ and $\text{Nd}^{10,13}$). The method is also in close accordance with the method given by Mehrotra et al. for the synthesis of several $\text{LnAl}_3(\text{OPr}^i)_{12}$, among which the Eu–Al 2-propoxide was reported.³¹ The structures of these molecules were not determined, but mass spectroscopy indicated the formula $\text{LnAl}_3(\text{OPr}^i)_{12}$.

The structural determination showed that **3** had formed, and the IR spectroscopic studies and the homogeneous color, shape, and Eu/Al ratio of the crystals indicated that the material was pure.

IR Spectroscopy. The IR spectrum of the alkoxide is shown in Figure 8; it is completely consistent with the IR spectra of other $\text{LnAl}_3(\text{OPr}^i)_{12}$ with $\text{Ln} = \text{Er},^{11} \text{Gd}$, and $\text{Nd}.$ ¹³ The great similarity of the IR spectra of the solid and the dissolved compound suggest that the molecular structure is retained to a large extent on dissolution in toluene/HOPrⁱ or hexane solvent.

UV–Vis Spectroscopy. The UV–vis spectra of the off-white solid and dissolved **2** are shown in Figure 9. The solid-state and hexane solution spectra are very similar, but differences, especially in the intensities, are shown for the HOPrⁱ-containing solution. This might indicate some changes

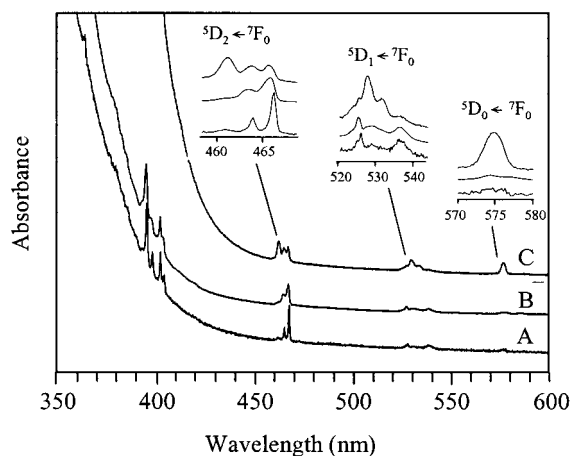


Figure 9. Electronic spectra of **3** as solid (A), hexane solution (B), and hexane/HOPrⁱ (1:1) solution (C).

in structure in the presence of the O-donor 2-propanol. The changes are probably small, because the peaks are found close to the hexane spectrum positions, while the other Eu 2-propoxides have quite different positions and intensities of the electronic transitions. A possible change could be that the Eu³⁺ ion coordinates an HOPrⁱ adduct and adopts seven-coordination. Such a structure was recently obtained by single-crystal X-ray determination for NdAl₃(OPrⁱ)₁₂(HOPrⁱ) by Veith et al, after crystallization from HOPrⁱ-containing solvent.³² On the other hand, we have obtained the non-solvated NdAl₃(OPrⁱ)₁₂ by crystallization from hexane/toluene.¹³ With the smaller radius of the Eu³⁺ ion, solvation should be more difficult than for the Nd³⁺ ion, but there is probably at least some tendency for adduct formation in these molecules in the presence of HOPrⁱ. Thus, it might be that a weak Eu³⁺⋯HOPrⁱ interaction influences the very sensitive Eu³⁺ probe.

Behavior on Heating. Visual inspection of crystals in melt-sealed glass capillaries showed no changes up to 104–105 °C, where they melted to yield a clear liquid. No further changes could be observed up to 300 °C. The DSC curve of **3** in Figure 3 shows an endothermic peak with onset at 102 °C and a minimum at 105 °C, fitting the melting point and corresponding to an energy of ~31 kJ mol⁻¹. This is in line with what was found for ErAl₃(OPrⁱ)₁₂ with a reproducible melting point at 120–122 °C.¹¹

Structure. In the solid state, **3** is isostructural with NdAl₃(OPrⁱ)₁₂¹³ and can be considered as a monoclinic deviation of the orthorhombic ErAl₃(OPrⁱ)₁₂.¹¹ The metal–oxygen framework of the molecular structure is shown in Figure 10, and selected bond distances are given in Table 4. The coordination polyhedron of the Eu atom can be described as twisted octahedral, that is, one triangular face of the octahedron is rotated through 28° around the 3-fold axis. The Eu–μ₂-O distances are narrowly distributed around 2.32 Å. The Eu and Al atoms are connected through μ₂-O bridges. Each Al atom has two additional terminal 2-propoxo oxygens completing the distorted tetrahedral coordination sphere. The Al–μ₂-O distances are approximately 0.10 Å longer than the terminal Al–O bonds. Furthermore, the Al–O–C angles at terminal O atoms are significantly smaller than the

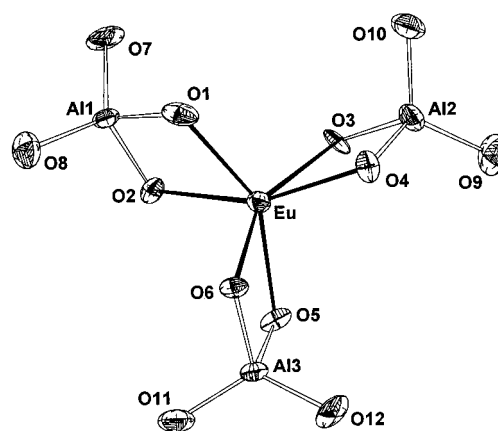


Figure 10. ORTEP view of the metal–oxygen framework of **3** showing 30% probability displacement ellipsoids.

Table 4. Selected Interatomic Distances (Å) for EuAl₃(OPrⁱ)₁₂ (**2**)

Eu(1)–O(1)	2.315(9)	Al(1)–O(8)	1.691(9)
Eu(1)–O(2)	2.335(7)	Al(2)–O(3)	1.833(9)
Eu(1)–O(3)	2.307(7)	Al(2)–O(4)	1.783(8)
Eu(1)–O(4)	2.342(9)	Al(2)–O(9)	1.693(10)
Eu(1)–O(5)	2.305(8)	Al(3)–O(10)	1.708(10)
Eu(1)–O(6)	2.318(7)	Al(3)–O(5)	1.803(8)
Al(1)–O(1)	1.823(11)	Al(3)–O(6)	1.801(8)
Al(1)–O(2)	1.787(8)	Al(3)–O(11)	1.700(11)
Al(1)–O(7)	1.684(8)	Al(3)–O(11)	1.712(9)

M–O–C angles found in f-element 2-propoxides, for example, **1** and **2**. The M–O bond distance distributions and calculated bond valence sum values indicate that the europium and aluminum atoms are all trivalent.

3.5 Reaction of Eu₅O(OPrⁱ)₁₃ (2**) and [Eu₄(OPrⁱ)₁₀(HOPrⁱ)₃]*2HOPrⁱ (**1**) with Al₄(OPrⁱ)₁₂.** We have studied the reaction of **2** and Al₄(OPrⁱ)₁₂ with a Eu/Al 1:3 ratio in toluene/HOPrⁱ (2:1 vol/vol) by UV–vis spectroscopy. In earlier articles, we have used the absorptions in the UV–vis–NIR region to follow alkoxide reactions in solution.^{9,10,15} Studies of the ⁵D₂ ← ⁷F₀, ⁵D₁ ← ⁷F₀, and ⁵D₀ ← ⁷F₀ transitions showed that the reaction was very slow at room temperature, and only small changes in the fine structure of **2** could be observed even after 24 h. At 75 °C, the reaction became much more rapid, and after 2 h, the fine structures of the peaks completely coincided with those of **3**, as shown in Figure 11. Evaporation of the solvent from this solution yielded a material homogeneous in Eu/Al ratio, according to SEM-EDS studies, and the IR spectrum was almost identical to that of **3**, as seen in Figure 12. Only one additional weak peak was found in the IR spectrum at 1005 cm⁻¹, whose origin is not known. Possibly, they might stem from a slightly erroneous Eu/Al ratio or the presence of small amounts of oxo or hydroxo groups. The latter might thus be an indication of where the oxo-oxygen of **2** ends up. At 90 °C, the reaction was even faster, being finished in about 1 h.

We have earlier studied the reactivity of Er₅O(OPrⁱ)₁₃, Nd₅O(OPrⁱ)₁₃, and Y₅(OPrⁱ)₁₃ with Al₄(OPrⁱ)₁₂ in the same way and obtained similar results, with times ranging from 2 to 3 h for complete conversion into MAl₃(OPrⁱ)₁₂ at 80 °C.^{9,10}

Reactivity of [Eu₄(OPrⁱ)₁₀(HOPrⁱ)₃]*2HOPrⁱ (1**) with Al₄(OPrⁱ)₁₂.** In the studies of the reaction between **1** and

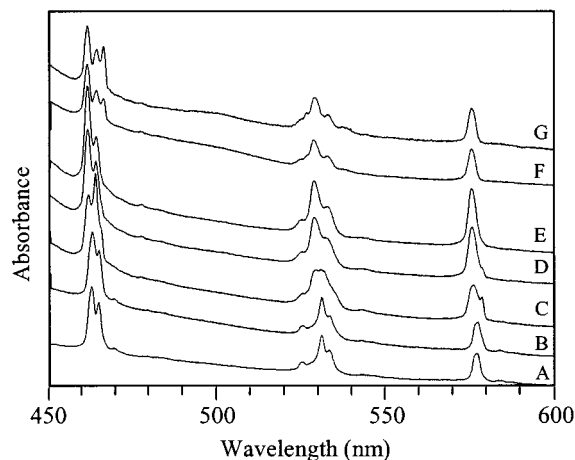


Figure 11. ${}^5D_2 \leftarrow {}^7F_0$, ${}^5D_1 \leftarrow {}^7F_0$, and ${}^5D_0 \leftarrow {}^7F_0$ transitions of Eu^{3+} in toluene/ HOPr^i (2:1) solutions of **2** (A); **2** and $\text{Al}_4(\text{OPr}^i)_{12}$ (Eu/Al 1:3) after 24 h at room temperature (B), 30 min at 75 °C (C), 60 min at 75 °C (D), 80 min at 75 °C (E), 120 min at 75 °C (F); and **3** (G).

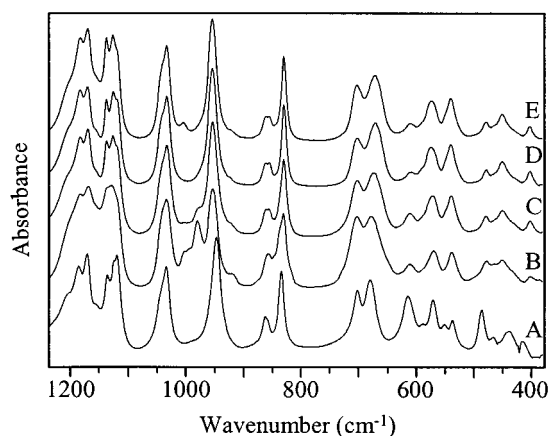


Figure 12. IR spectra of $\text{Al}_4(\text{OPr}^i)_{12}$ (A); a mixture **1** and $\text{Al}_4(\text{OPr}^i)_{12}$ with an Eu/Al ratio of 1:3 after heating in toluene/ HOPr^i (2:1) at 75 °C for 2 h and evaporation of solvent, the bright yellow, viscous liquid (B), and the off-white crystals (C); **3** (D); and the solid obtained after heating in toluene/ HOPr^i (2:1) of a mixture of **2** and $\text{Al}_4(\text{OPr}^i)_{12}$ (Eu/Al 1:3) at 75 °C for 2 h, after evaporation of solvent (E).

$\text{Al}_4(\text{OPr}^i)_{12}$ with a Eu/Al ratio of 1:3 in toluene/ HOPr^i solvent, only the ${}^5D_1 \leftarrow {}^7F_0$ and ${}^5D_0 \leftarrow {}^7F_0$ transitions of the Eu^{3+} ion could be observed because of the low intensity of the peaks. At room temperature, some reaction took place, causing changes in the peaks due to Eu^{3+} , while the solution clearly still contained a large amount of Eu^{2+} , observable as the strong band tailing in from shorter wavelengths, yielding the strong yellow color. The new peaks corresponded better to **2** than to **3**, as can be seen in Figure 13. If **2** is formed, it might be because the Eu^{2+} ions react to form a new compound, possibly with $\text{Al}_4(\text{OPr}^i)_{12}$, leaving the Eu^{3+} ions to form the more stable compound **2**. The IR spectrum showed peaks mainly from $\text{Al}_4(\text{OPr}^i)_{12}$ which gives rise to strong peaks in the IR spectrum, and the remaining peaks could not be identified. At 75 °C, the reaction proceeded to a steady state after 2 h, with peaks in the UV–vis region of the same shape and position as for dissolved **3**. From the remaining strong yellow color, it seems that the Eu^{2+} ions introduced through **1** remained in the solution. Evaporation of the solution yielded an inhomogeneous material, from

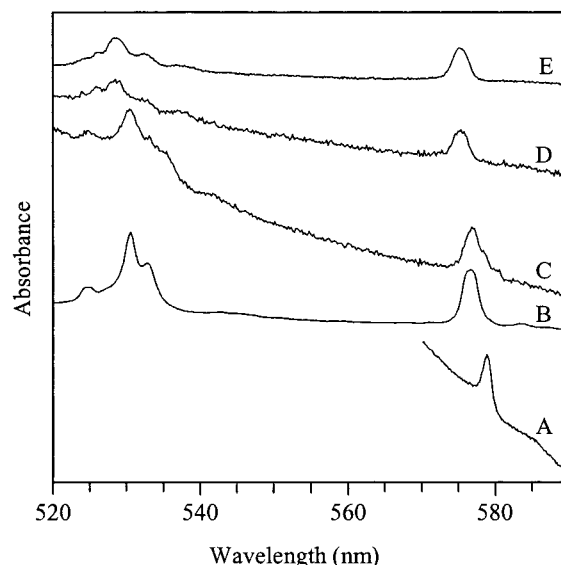


Figure 13. Electronic spectra of Eu^{3+} obtained of **1** (in HOPr^i) (A); **2** (in toluene) (B); a mixture of **1** and $\text{Al}_4(\text{OPr}^i)_{12}$ (Eu/Al 1:3) after 24 h at room temperature (C), 120 min at 75 °C (D); and **3** (E), all in toluene/ HOPr^i (2:1).

which off-white crystals were obtained in about 50% yield, which showed an IR spectrum very similar to that of **3**; only a small additional shoulder was found at $\sim 970 \text{ cm}^{-1}$, which might stem from the other part of the material which was a bright, yellow, viscous liquid. There seemed to be no $\text{Al}_4(\text{OPr}^i)_{12}$ left according to the IR spectrum, which suggests that the viscous liquid was essentially a Eu^{2+} –Al alkoxide. At 90 °C, the reaction was complete with the same results as for the 75 °C study after 1 h, similar to the **2**– $\text{Al}_4(\text{OPr}^i)_{12}$ mixture. A possible interpretation of these results is then that first the Eu^{2+} ions react to form an Eu^{2+} –Al alkoxide, and then the remaining Eu^{3+} ions yield **2**. The latter alkoxide then reacts with $\text{Al}_4(\text{OPr}^i)_{12}$ within 2 h, following the results reported for **2**.

4. Conclusions

Three Eu 2-propoxides have been prepared, their structures determined, and their reactivities studied. $[\text{Eu}_4(\text{OPr}^i)_{10}(\text{HOPr}^i)_3] \cdot 2\text{HOPr}^i$ (**1**) was obtained by dissolution of Eu metal at temperatures from 25 to 70 °C in toluene/ HOPr^i solvent. It turned out to be a mixed $\text{Eu}^{2+}/\text{Eu}^{3+}$ compound, contrary to what has been believed. The butterfly-shaped tetranuclear molecular units contained a very rare example of μ_4 -OR groups, which is also the first such group with $\text{R} = \text{OPr}^i$.

Combined metathesis with EuCl_3 and KOPr^i and stoichiometric hydrolysis produced the exclusively Eu^{3+} ion containing alkoxide, $\text{Eu}_5\text{O}(\text{OPr}^i)_{13}$ (**2**), which has the same square pyramidal molecular structure as the other $\text{M}_5\text{O}(\text{OPr}^i)_{13}$ compounds reported, with the oxo-oxygen atom slightly above the basal plane.

Conversion of **1** to **2** was possible by oxidation of **1** with oxygen gas, while reduction with Eu metal of **2** did not yield **1**.

Metathesis with EuCl_3 and $3\text{KAl}(\text{OPr}^i)_4$ yielded $\text{EuAl}_3(\text{OPr}^i)_{12}$ (**3**), which has the same structure as the earlier determined $\text{LnAl}_3(\text{OPr}^i)_{12}$ ($\text{Ln} = \text{Er}, \text{Nd}$). Compound **3** can also be obtained by reaction of **2** and $\text{Al}_4(\text{OPr}^i)_{12}$ at 75°C . This is in accordance with our previous results with $\text{Ln} = \text{Y}, \text{Er}, \text{Gd},$ and Nd but contradicts the reports on this reaction with $\text{Ln} = \text{Y}, \text{Nd},$ and Sc from other groups. This reaction is of importance, not only for the understanding of alkoxide chemistry, but also because $\text{LnAl}_3(\text{OPr}^i)_{12}$ is a very good precursor to Ln-doped lasing waveguides via sol-gel or CVD processing, because clustering of Ln ions in the oxide

matrix severely reduces the optical yield in the important laser applications.

Acknowledgment. The natural science research council (NFR) has financed this work. Dr. K. Jansson, Stockholm University, is thanked for performing the DSC measurements.

Supporting Information Available: X-ray crystallographic files in CIF format for complexes **1**, **2**, and **3**. This material is available free of charge via the Internet at <http://pubs.acs.org>.

IC010745L